Cellular and Molecular Life Sciences (2019) 76:1605–1621
https://doi.org/10.1007/s00018-019-03013-8

ORIGINAL ARTICLE

Cellular responses to proteostasis perturbations reveal non-optimal feedback in chaperone networks

Asmita Ghosh[1,2] · Abhilash Gangadharan[1,2] · Monika Verma[1,2] · Sarada Das[3] · Latika Matai[1,2] · Devi Prasanna Dash[1,2] · Debasis Dash[1,2] · Koyeli Mapa[3] · Kausik Chakraborty[1,2]

Received: 14 September 2018 / Revised: 10 January 2019 / Accepted: 15 January 2019 / Published online: 25 January 2019

Abstract

The proteostasis network (PN) comprises a plethora of proteins that are dedicated to aid in protein folding and maintenance; some with overlapping functions. Despite this, there are multiple pathophysiological states associated with depletion of chaperones. This is counter-intuitive, assuming cells have the ability to re-program transcriptional outputs in accordance with its proteostasic limitations. Here, we have used *S. cerevisiae* to understand how cells respond to different types of proteostasis impairments. We monitored the proteostasis status and transcriptome of single deletions of fourteen different Protein Quality Control (PQC) genes. In most cases, cellular response did not activate proteostasis components or pathways that could either complement the function of the missing PQC gene or restore proteostasis. Over-expression of alternate machineries could restore part of the proteostasis defect in two representative PQC gene deletion strains. We posit that *S. cerevisiae* inherently lacks the ability to sense and respond optimally to defects in proteostasis caused due to deletion of specific PQC components.

Keywords Chaperones · Transcriptomics · Epistasis · Proteostasis · *S. cerevisiae*

Introduction

A nascent polypeptide chain emerges from the ribosome as a linear chain of amino acids. Most nascent chains need to fold into its specific three-dimensional structure to attain its function. The exception to this being the proteins with intrinsically disordered regions that remain in a flexible, semi-unfolded state [1, 2]. To navigate from an unfolded, linear chain to its specific three-dimensional structure without misfolding, the cell has a complex network of proteins which assist with either co-translational and or post-translational folding to reach the native structures [3, 4]. Further downstream, other proteins assist in translocation, cellular localization and eventually degradation [5–7]. The collective group of chaperones, co-chaperones and degradation proteins that coordinate these processes are considered to constitute the Protein Quality Control (PQC) system and are integral nodes in the Proteostasis Network (PN) [8, 9]. While proteins are helped by the PQC machinery to attain and maintain their native states, what happens if a PQC component is rendered functionally defective?

There are ample evidences in the literature showing multiple phenotypes associated with various pathological conditions that are known to occur due to chaperone depletions. Mutations in the coding region of chaperones that compromises its function, result in a disease phenotypes defined as chaperonopathy [10]. Even otherwise, chaperones can be depleted in a cell when they are over-burdened with an excessive load of misfolded or aggregated proteins. For instance, polyglutamine (polyQ) aggregates sequesters Sis1 [11], while Aha1 engages extensively with misfolded

Electronic supplementary material The online version of this article (https://doi.org/10.1007/s00018-019-03013-8) contains supplementary material, which is available to authorized users.

Asmita Ghosh and Abhilash Gangadharan are equally contributing first authors. Kausik Chakraborty, Koyeli Mapa and Debasis Dash are equally contributing senior authors.

✉ Kausik Chakraborty
kausik@igib.in

[1] CSIR-Institute of Genomics and Integrative Biology, Delhi 110025, India

[2] Academy of Scientific and Innovative Research, Coordination Office, CSIR-Human Resource Development Centre Campus, Ghaziabad 201002, India

[3] Department of Life Sciences, School of Natural Sciences, Shiv Nadar University, Greater Noida 201314, India

A. Schematic of the localization and function of the different PQC genes that are used in this study

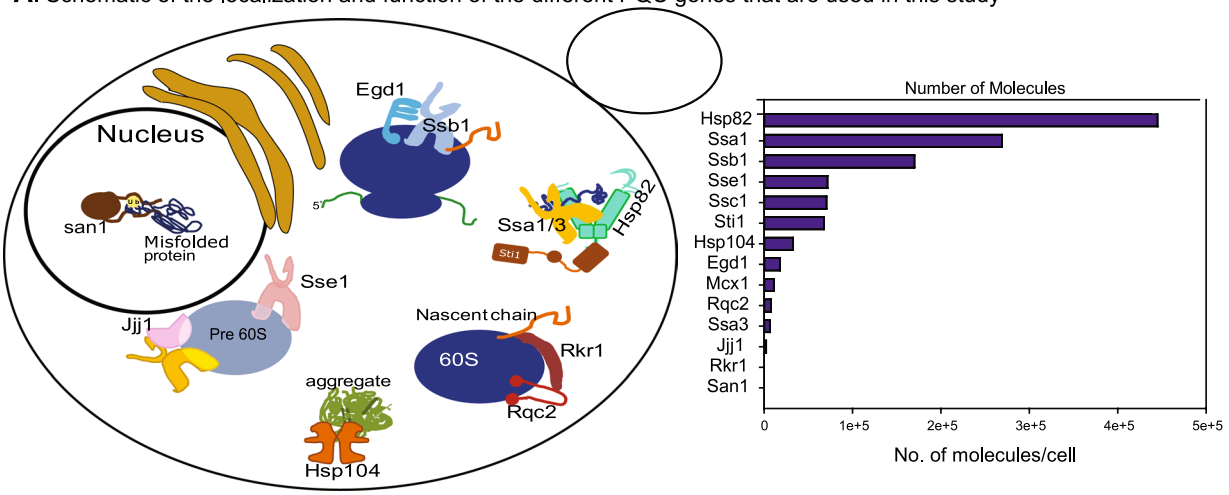

B. Fitness defects of different PQC Δ strains at 30°C

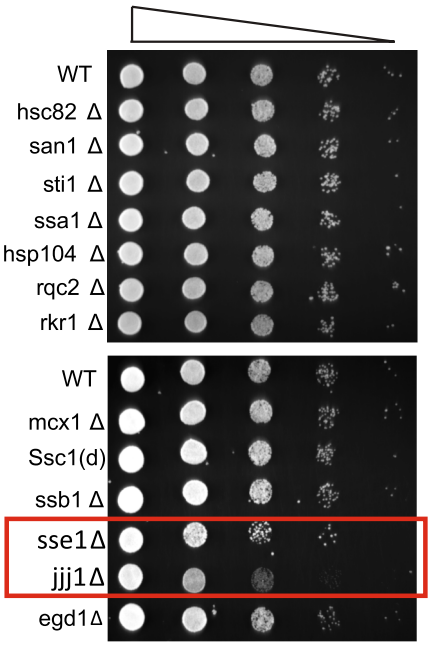

C. Fitness defects of different PQC Δ strains at 37°C

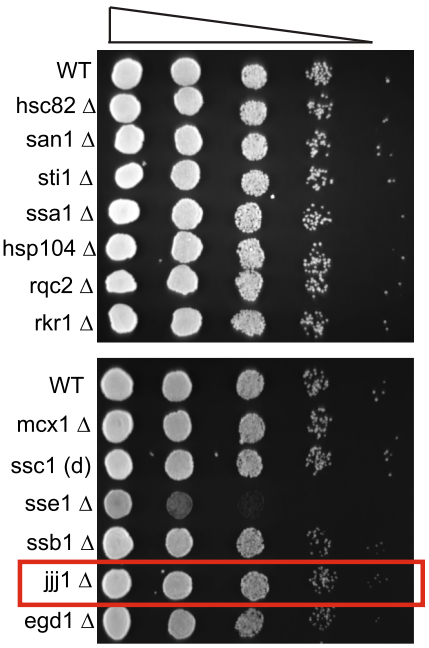

D. Fitness defects of the different PQC gene Δ strains with AZC

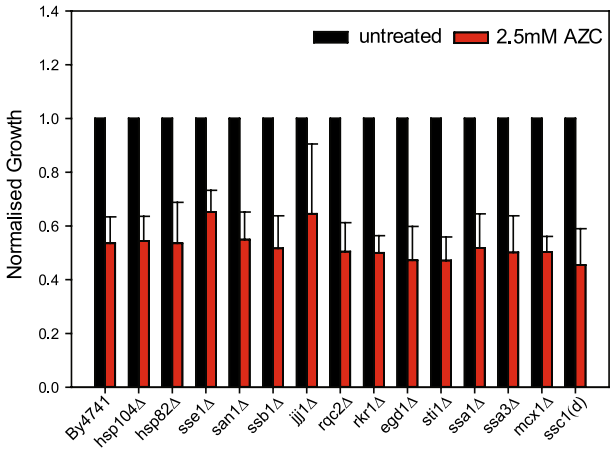

◂**Fig. 1** **a** Left panel shows localisation and function of each of the PQC genes we picked for the study in the schematic. The right panel shows number of molecules/cell for the selected PQC components as reported by Ghammaghemi et al. [23]. **b** The deletion (and depletion) strains were spotted on YPD agar plates at 30 °C to assay growth fitness of the strains. **c** The deletion (and depletion) strains were spotted on YPD agar plates at 37 °C to assay growth defect of the strains upon chronic heat stress. **d** The deletion (and depletion) strains were grown for 12 h with or without L-AZC at 30 °C to assay growth defect of the strains upon chronic misfolding stress ($n=3$)

CFTR Δ508, thus being unavailable to help fold its normal repertoire of substrates [12, 13].

Given the redundancies present in the PQC genetic network and the large number of inter-connected components [14], the PN is expected to adapt to altered demands and depletion of PQC nodes through the stress response pathways. This is counter-intuitive when one considers the preponderance of protein aggregation associated phenotypes and diseases [15]. Polyglutamine (polyQ) aggregates have been shown to prevent Hsf-1 mediated heat shock response in mammalian systems [16, 17]. This has led to the proposal that polyQ aggregates may be toxic as it renders cells incapable of responding optimally to proteotoxicity [18, 19]. However, this is based on the assumption that in the absence of polyQ aggregates, the cells are capable of sensing and responding optimally to other types of proteotoxic challenges or PQC component depletions. We therefore asked if cells have the capability to reorganize their PN optimally during proteotoxic challenge in the absence of any polyQ or similar proteinopathic aggregates. To perturb PN in the absence of any exogenous misfolding and polyQ proteins, we used single deletions of different PQC nodes to challenge cellular proteostasis. We chose to delete single genes as there was not an endogenous way to perturb only one node without affecting other hubs; primarily due to a lack of well-defined substrate exclusivity.

There are three plausible ways in which a cell may respond to PQC gene depletions. First, it may sense the loss of function of client proteins as the cognate chaperone is depleted. In this case, cells would try to upregulate genes to take care of cellular pathways that are compromised due to non-folding of client proteins. Second, misfolding or aggregation of substrate proteins can be toxic and cells may induce transcription of the stress response system to upregulate the entire cohort of chaperones and degradation machineries. Third, the cell can sense the loss of specific PQC node and upregulate the existing compensatory or paralogous pathways to take care of the depletion [20, 21]. We still do not know the preferred route of cellular response to depletion of specific nodes of the PQC.

We obtained the transcriptome of a repertoire of 14 PQC gene deletions in *S. cerevisiae* where different modules of the PN are perturbed. Chaperones to be deleted were chosen to represent the diverse hubs that govern proteostasis in *S. cerevisiae* (Fig. 1a, left panel). Ssa1 was chosen as the most canonical and constitutively present Hsp70 while Ssa3 being the inducible Hsp70 chaperone in the cytosol [20]. Hsp82 and its co-chaperone Sti1 represent the cytosolic Hsp90 system. Hsp104 as a disaggregase and San1, an E3-ligase as part of protein degradation machinery. The other classes of proteostatic components selected in our study were primarily involved in ribosome-associated quality control (Rqc2, Rkr1), ribosome-associated folding of nascent chains (Ssb1, Egd1) [3], and ribosome assembly (Sse1, Ssb1, Jjj1) [22]. Deletion of mcx1 and a hypomorphic allele of ssc1 (DAMP allele) were used to obtain information pertaining to the cellular response due to the loss of mitochondrial chaperones. The abundance of each of these proteins varies (Fig. 1a, right panel) under basal conditions in a wild-type strain [23]; this provides an insight into house-keeping load that is shared by a particular PQC in the cell.

In this work, we show that deletion of protein quality control hubs led to an underlying loss of proteostasis although without any overt fitness defect during normal growth or during proteotoxic stress. Remarkably, it appears that even a phenotypically healthy and exponentially growing cell had underlying proteostasis defects. Analysing the response in light of known gene–gene interaction network, we found that the redundant machineries were not specifically upregulated in most deletions. Using two examples, sse1Δ and jj1Δ, we found that activating a parallel pathway exogenously help cells over-come proteostasis defect resulting from the absence of these PQC component. Thus, it appears that in the PN, *S. cerevisiae* cells inherently have a limited optimality as they are unable to compensate for the lost PQC nodes by inducing compensatory pathways.

Results

PQC deletions have compromised proteostasis

We measured growth of the chosen PQC deletion (and depletion) strains and found only sse1Δ and jjj1Δ to have a defect at 30 °C (Fig. 1b). Most of the deletion strains did not show a growth defect at 37 °C, a mild heat shock condition (Fig. 1c), or in AZC (Fig. 1d) that induces misfolding stress. sse1Δ was the only strain that showed more growth defect at 37 °C than at 30 °C. Surprisingly, the other PQC deletions did not have a drastic impact in cellular fitness even during misfolding stress indicating that either the deleted chaperones played only a minor role, or cellular readjustment near-perfectly solved the problem arising from the deletion.

To check if cellular readjustment restored proteostasis in the deletion strains, we required a sensor of cellular proteostasis. We designed this using the Nourseothricin Acetyl

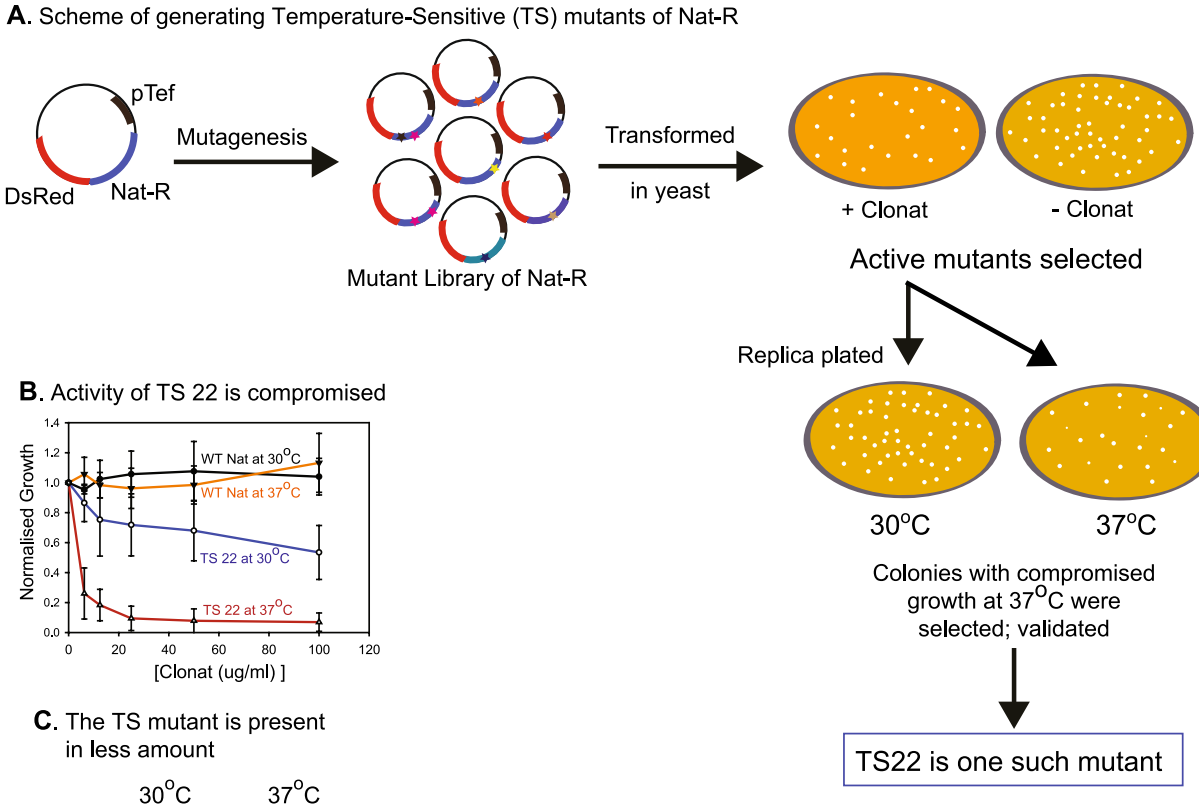
A. Scheme of generating Temperature-Sensitive (TS) mutants of Nat-R
pTef
DsRed
Nat-R
Mutagenesis
Mutant Library of Nat-R
Transformed
in yeast
+ Clonat
- Clonat
Active mutants selected
Replica plated
30°C
37°C
Colonies with compromised growth at 37°C were selected; validated
TS22 is one such mutant

B. Activity of TS 22 is compromised
Normalised Growth
WT Nat at 30°C
WT Nat at 37°C
TS 22 at 30°C
TS 22 at 37°C
[Clonat (ug/ml)]

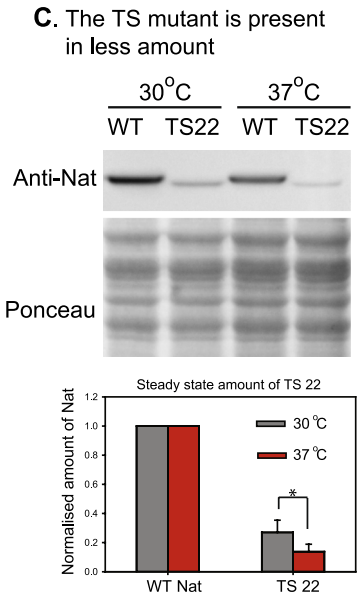
C. The TS mutant is present in less amount
30°C
37°C
WT
TS22
WT
TS22
Anti-Nat
Ponceau
Steady state amount of TS 22
Normalised amount of Nat
30 °C
37 °C
WT Nat
TS 22

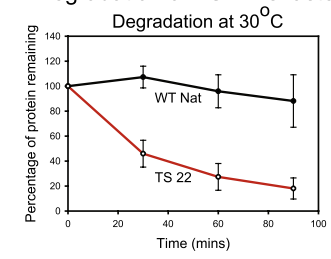
D. Degradation of TS 22 is faster
Degradation at 30°C
Percentage of protein remaining
WT Nat
TS 22
Time (mins)

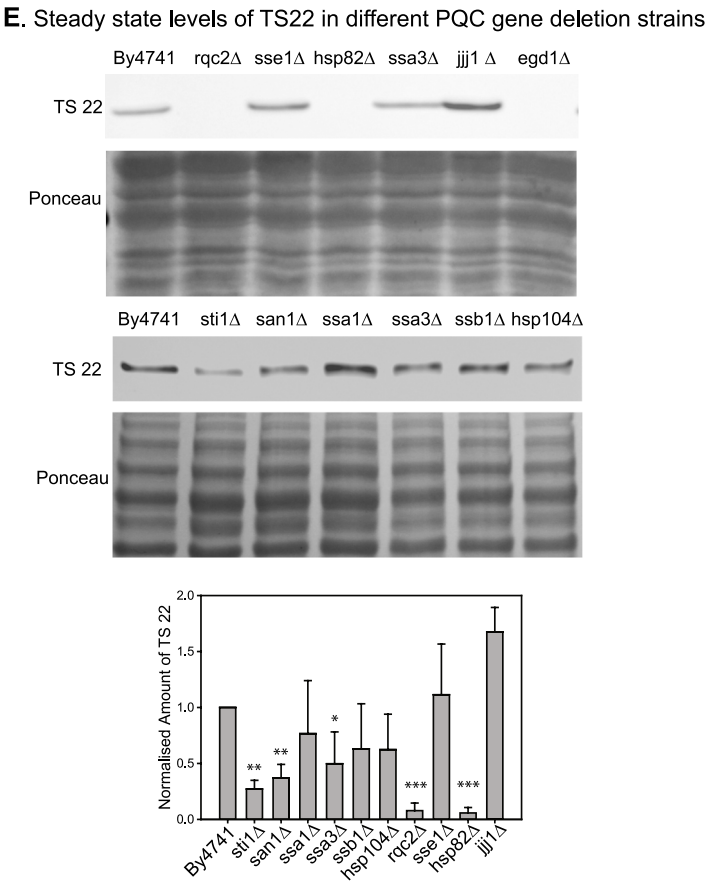
E. Steady state levels of TS22 in different PQC gene deletion strains
By4741
rqc2Δ
sse1Δ
hsp82Δ
ssa3Δ
jjj1 Δ
egd1Δ
TS 22
Ponceau
By4741
sti1Δ
san1Δ
ssa1Δ
ssa3Δ
ssb1Δ
hsp104Δ
TS 22
Ponceau
Normalised Amount of TS 22
By4741
sti1Δ
san1Δ
ssa1Δ
ssa3Δ
ssb1Δ
hsp104Δ
rqc2Δ
sse1Δ
hsp82Δ
jjj1Δ

◂**Fig. 2** **a** Schematic showing the generation of TS mutants of Nat. Multiple mutants were isolated, but only TS22 was used for this study as a candidate metastable protein. **b** Growth assay of WT Na-Rt and TS22 with varying concentrations of the antibiotic nourseothricin (Clonat) at 30 °C and 37 °C to assay for the functionality of the proteins in vivo. **c** Steady state amounts of WT Nat-R and TS22 at 30 °C and 37 °C were determined by western blot analysis ($n=3$). **d** The stability of WT Nat-R and TS22 was determined following a cycloheximide chase at 30 °C. Ponceau was used for normalisation of protein per lane (loading control) ($n=3$). **e** Representative blots for steady state amounts of TS22 at 30 °C in different PQC gene deletion strains were determined by western blot analysis. Ponceau was used for loading normalisation. The graph at the bottom shows quantification from three biological replicates. In all figures, $*p<0.05$, $**p<0.01$, $***p<0.001$

Transferase gene (Nat-R). We made several temperature sensitive (TS) mutants of this protein in *S. cerevisiae* by screening for resistance to CloNAT (an antifungal/antibiotic) at 37 °C (restrictive temperature) and 30 °C (Fig. 2a). TS22 was a strong temperature sensitive mutant of Nat-R (Fig. 2b, c) and degraded faster than WT Nat-R protein even at 30 °C (Fig. 2d, S1A), although mere presence of this mutant did not confer any growth defect to the cells (Fig. S1B). This mutant was indeed sensitive to proteostasis alterations as the steady state protein level decreased in the presence of heat shock response inducing compound, celastrol, that changes the chaperone pool and hence proteostasis. WT Nat-R protein was not similarly affected (Fig. S1C).

We used this sensor to monitor the state of proteostasis in the deletion strains (Figs. 2e; S1D–F) by measuring the steady state amount of TS22 with respect to WT Nat-R protein expression in the same strains. jjj1Δ was special as it exhibited increase in both WT Nat-R and TS22 levels, indicating an increase in transcription or translation of the gene product. The in vivo activity of Nat-R (and mutants) was measured by the ability of the cells expressing the protein to growth in the presence of increasing concentrations of the antibiotic Nourseothricin or CloNat. Comparative growth assays for TS22 and WT Nat-R in BY4741 and the PQC deletion strains show that the TS22 (but not of WT Nat-R) has lower activity in the PQC deletion strains (S1G) compared to their activity in BY4741. Thus, PQC deletion strains indeed had a problem in maturation of the metastable form of the protein.

We also used TS mutants of yeGFP (referred to as GFP here onwards) as sensors of proteostasis to examine the generality of our finding with TS mutants of Nat-R. We isolated two different mutants (M1, M8) of yeGFP that showed less fluorescence than WT GFP (Fig. 3a) under basal conditions. These mutants of GFP had extremely low fluorescence upon heat stress at 37 °C (Fig. 3b), making them TS mutants. We confirmed that expression of these mutants in BY4741 did not confer any growth defect (Fig. 3c) when grown at 30 °C, despite being expressed from a constitutive promoter, glyceraldehyde-3-phosphate dehydrogenase (GAPDH/GPD). When we expressed these mutants in PQC deletion strains, we found the GFP mutants to have significantly lower fluorescence in PQC deletion strains than in BY4741 (Fig. 3d). While M1 and M8 could report changes in proteostasis conditions, they were not as sensitive as TS22. Taken together, most of the PQC gene deletion strains did not show a strong phenotype upon chronic heat shock or upon AZC treatment. However, these strains have defective proteostasis as inferred from decreased levels of a metastable sensor protein, TS22 as well as lower fluorescence of M1 and M8 GFP mutants in these PQC deletion strains. This suggests that although there is a dysfunction of general proteostasis in these deletion strains, cells lack the ability to sense it and upregulate the necessary restorative pathways. These results led us to ask how cells respond to these deletions, and why is this not sufficient to restore proteostasis.

Response to PN pertubations is independent of heat shock response

Towards this we asked if the cells sensed the absence of the PQC component and mounted any response. Since most of the chosen PQCs were cytosolic, we checked for the reported effect of these deletions on the heat shock response (HSR), the canonical cytosolic stress response pathway [24]. Analysis of the published result using HSR reporter, HSE-GFP show that some of the strains such as sse1Δ, hsp104Δ, sti1Δ have high basal HSR (at 25 °C), due to the deletion of the chaperones. (Fig. S2A). However, strains such as hsp82Δ, jjj1Δ that do not have any HSE-GFP fluorescence at 25 °C; indicate they do not have any basal HSR due to the chaperone deletion. This does not exclude such strains such as hsp82Δ, jjj1Δ from losing the ability to mount HSR at all, as these very strains are able to induce a HSR upon heat shock at 37 °C. Whether a strain has basal HSR (such as sse1Δ) or not (such as hsp82Δ), they still have an underlying proteostatic defect as observed by lower amounts of a metastable protein, either TS22 (Figs. 2e; S1E and S1F) or M1-GFP (Fig. 3d). From this, we reflect that the cellular response observed thus, could be the result of upregulation of genes to tackle the functionality of possibly non-functional proteins (primarily the client proteins) arising due to depletion of the PQC gene in question. To obtain a global view of cellular response, we carried out RNA-sequencing based transcriptomics for the 14 PQC gene deletion strains in duplicates (Tables S1 and S2). Unlike the synthetic HSR reporter, the expression levels of the canonical Hsf1-dependent HSR-gene ssa4 were high in only sse1Δ. But the expression level of hsp12, a Msn2/4 reporter, was high in most of the PQC deletions (Fig. S2B). This categorically negates the possibility that the deletions did not alter cellular homeostasis. There is indication of stress upon depletion of each of the PQCs,

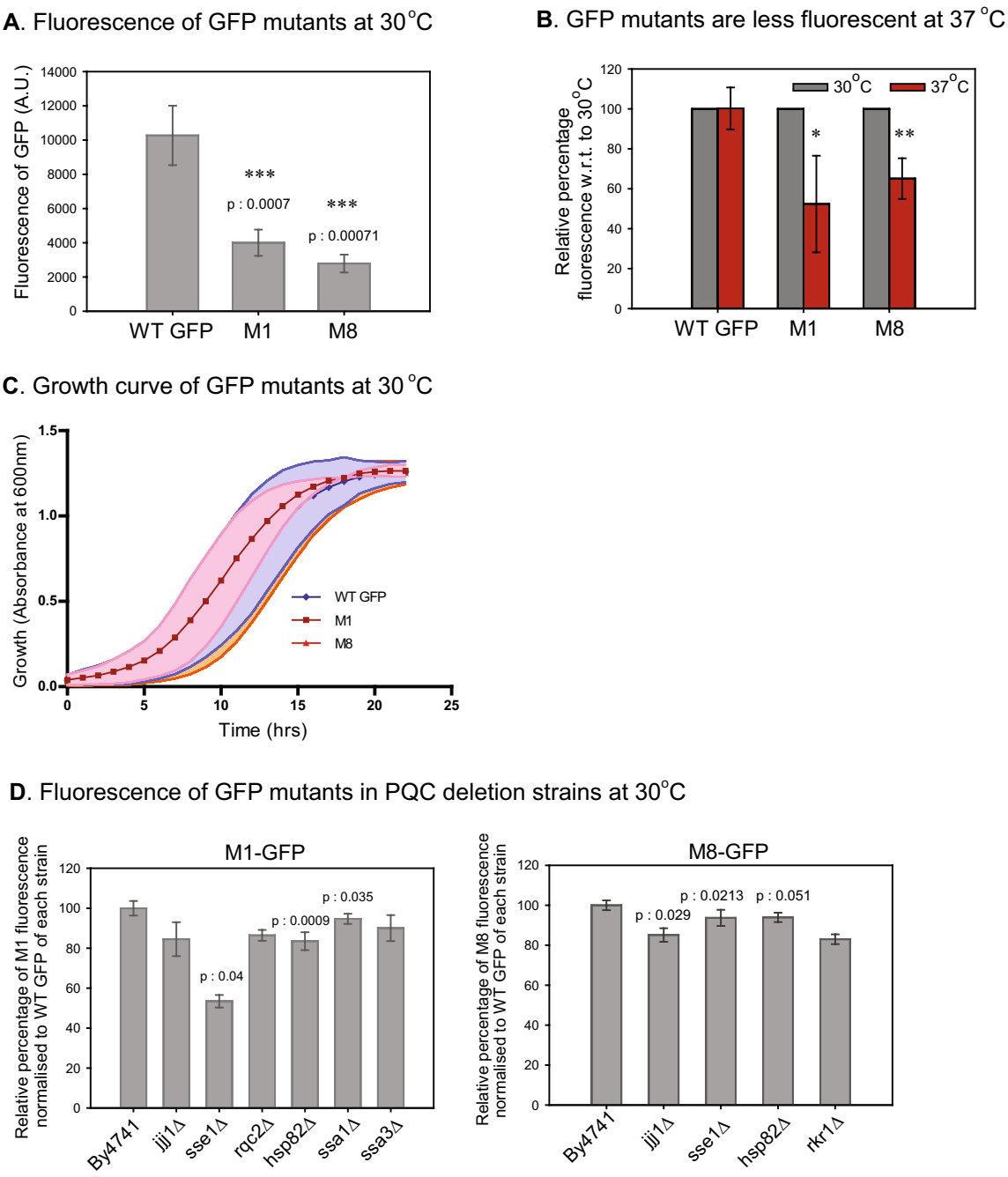

Fig. 3 **a** Fluorescence of GFP in BY4741 quantified by flow cytometry. Relative percentage fluorescence of M1 and M8 as compared to WT GFP when grown at 30 °C is shown. ($n=4$). **b** Fluorescence of GFP in BY4741 grown at 30 °C or at 37 °C was quantified by flow cytometry and plotted. Relative percentage fluorescence of GFP as compared to their respective 30 °C counterparts is plotted ($n=4$). **c** Growth curve of WT GFP, M1 and M8 in BY4741 is shown, when grown at 30 °C in Bioscreen. The mean is plotted as the line with symbols and the standard deviation arising due to variability from three independent biological replicates are shown as coloured error bands. **d** Relative percentage fluorescence of M1 GFP (left panel) and M8 (right panel) in PQC deletion strains, normalized to their respective WT GFP fluorescence is plotted. ($n=4$). In all figures, $*p<0.05$, $**p<0.01$, $***p<0.001$

the cells sense this and upregulate Msn2/4 pathway and in the case of sse1Δ, the Hsf1 pathway.

Although there is indication of altered proteostasis and cellular response to stress, it was surprising that lack of abundant chaperones such as Ssa1 or Hsp82 did not induce the expression of ssa4. Hsf1 regulates ssa4 expression, and Hsf1 is thought to be the canonical sensor for altered cytosolic proteostasis in eukaryotes. Importantly, the canonical

HSR genes are not enriched in the set of upregulated genes in the PQC deletions (Fig. S2C). While the HSR genes were not downregulated either in these PQC perturbation strains, the lack of a strong HSR indicates (Table S3) that the general response to PQC deletions does not induce a canonical HSR in *S. cerevisiae* as might be expected. Surprisingly, none of the strains show a significant increase in overall chaperone levels (Table S2).

We asked if the magnitude of response to deletion of a PQC gene is correlated to the expected load on that PQC component node. The load can be approximated by the physiological protein concentration of each of the PQC components. To obtain the total magnitude of cellular perturbation upon deletion of a PQC node, we took two approaches. First, we measured the total number of differentially regulated genes when a PQC is deleted. Second, we measured the divergence of the transcriptome of a PQC gene deletion strain with respect to WT cells (Table S4). Both these measures of magnitude of response did not correlate with the copy number of the deleted PQC protein (Fig. 4a, b). For example, protein copy of Ssa1 is higher than Sse1, yet deletion of sse1 causes a larger transcriptome reorganization than ssa1 deletion.

It was possible that the cellular response to PQC gene depletion was initiated either by loss-of-function of clients, or by proteotoxicity arising from misfolded proteins. Aiming to segregate the effects, we characterized the responses in terms of proteostasis components that are differentially expressed in these PQC deletions. The divergence of proteostasis components from the WT cells (BY4741) were generally low compared to the rest of the genes (Fig. 4c; Tables S4, S5), indicating that proteostasis components were on an average less perturbed than other cellular components upon PQC deletion. We compared the mean divergence of all the proteostasis network genes to that of divergence of a random set of same number of genes. Surprisingly, we find that there is less of alteration in the expression of the proteostasis genes upon PQC deletion. This was unexpected as one would assume that the cell would try to upregulate the proteostasis genes to combat the deficiency in maintaining proteostasis arising due to PQC depletion. However, this explains why we find lowered activity of a metastable protein TS22 (Fig. 2e) as well as reduced fluorescence of M1 and M8 GFP mutants (Fig. 3d) in the PQC deletion strains. Proteasome/protein clearance pathways are the only ones related to proteostasis that are consistently, but mildly, upregulated in many strains (Fig. 4d; Table S6). This indicated that the response was most probably dominated by the effect of non-functional client proteins and not by the toxicity of misfolded or aggregate proteins. This corroborates nicely with the absence of Hsf1 dependent signal. If the cells were able to sense an aberration in its proteostatic capacity, then we would have found upregulation of chaperones under the control of HSF1, the primary transcription factor for cytosolic misfolding stress to restore the proteostasis capacity. As we do not find activation of the HSF1-axis in most strains, it also explains the loss of proteostasis capacity as measured by the sensor, TS22 (Fig. 2e; S1F, G) as well as M1 and M8 (Fig. 3d). From this, we reflect that the observed cellular response could be to tackle non-functional proteins (primarily the client proteins) arising due to the particular PQC depletion. Interestingly, jjj1Δ and sse1Δ show the highest perturbation in proteostasis genes according to this measure suggesting that these strains have the largest proteotoxicity dependent response; these strains are also the only ones that show a measurable growth defect.

Taken together, each of the PQC deletions reorganize their transcriptome sensing some stress; the reorganization is, however, not dependent upon the canonical heat shock pathway. There is an elemental proteostasis deficiency upon PQC component depletion that is evident with lowered amounts and decreased activity of TS22 in most of these deletion strains. Despite this underlying deficiency, we find that the cells do not upregulate canonical stress response pathways. We speculate that the response thus seen, results from the cells trying to cope with the loss-of-function of proteins that were dependent on these PQC genes (possibly client proteins of these chaperones). However, there is a mild misfolding stress that in many cases is dependent on the Msn2/4 axis, but overall, the response is not correlated to the expected load on the deleted node of PQC.

Basis of cellular response to chaperone deletion

If the response primarily is the result of loss-of-function of client proteins, deletion of chaperones that have overlapping substrates should up- or down-regulate similar genes. To check similarities between the responses of two different deletion strains, we obtained the pairwise correlation coefficients between the transcriptome profiles of different chaperone deletion strains (Figure S3A). This was done by plotting the correlation between the transcriptome profiles (fold-change values of a chaperone deletion with respect to WT). The strength of the correlations indicates similarity between the responses of two chaperone deletions. A hierarchical clustering of the correlation matrix (Fig. 5a) also depicted similarities in the transcriptomic response that was apparent within multiple chaperones. Hierarchical clustering identified four main clusters in the plot. First, a cluster of two cytosolic (Jjj1, Ssa1), and two mitochondrial (Mcx1, Ssc1) PQC nodes were formed (cluster 1). Second, the more heterogeneous group consisting of chaperones (Sti1, Hsp82, Ssb1) along with two E3 ubiquitin ligases (Rkr1, and San1) (cluster 2). Co-clustering of San1 and Rkr1 along with other chaperones, highlight the importance of these two proteins in proteostasis maintenance in

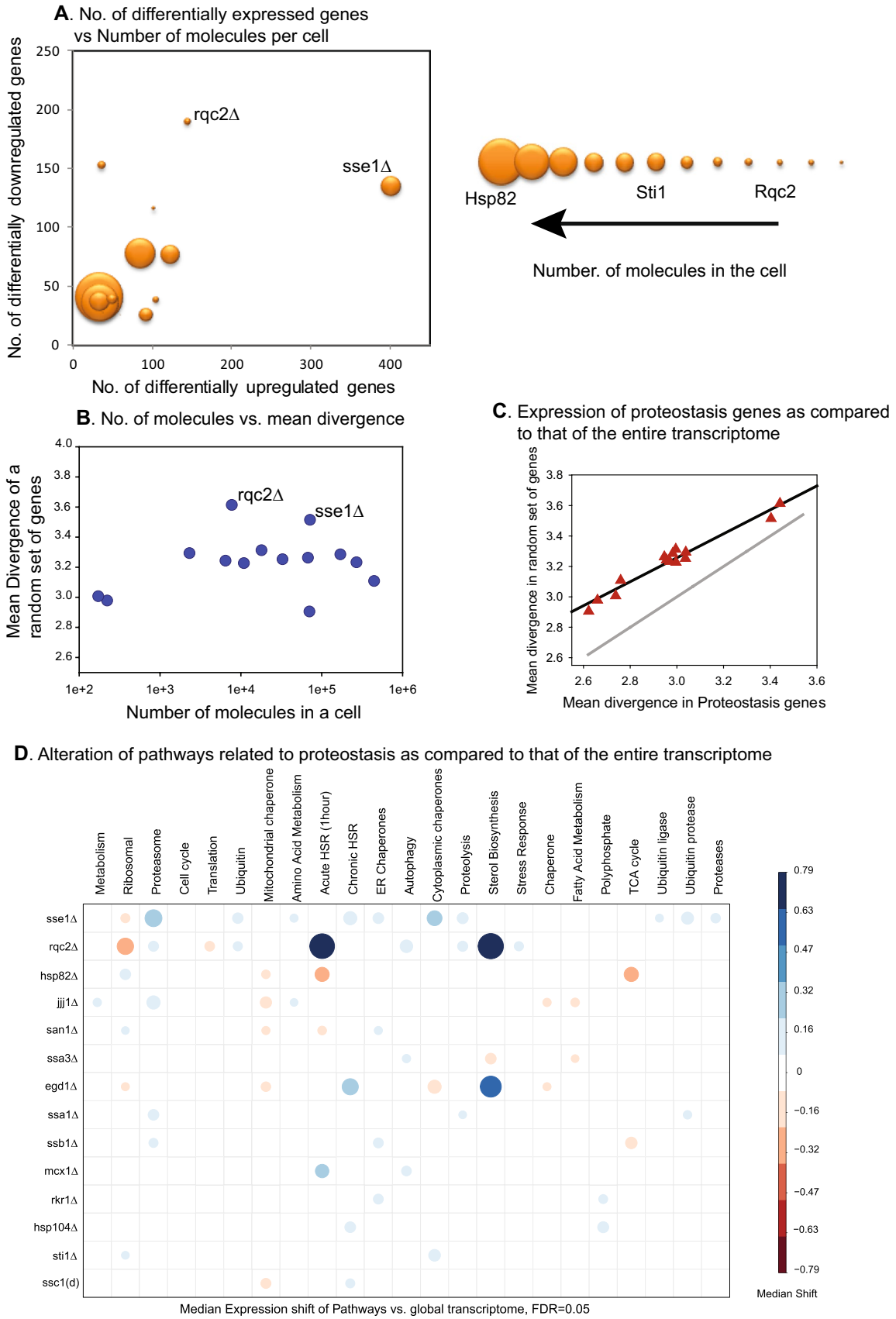
A. No. of differentially expressed genes vs Number of molecules per cell
No. of differentially downregulated genes
No. of differentially upregulated genes
rqc2Δ
sse1Δ
Hsp82
Sti1
Rqc2
Number. of molecules in the cell
B. No. of molecules vs. mean divergence
Mean Divergence of a random set of genes
Number of molecules in a cell
C. Expression of proteostasis genes as compared to that of the entire transcriptome
Mean divergence in random set of genes
Mean divergence in Proteostasis genes
D. Alteration of pathways related to proteostasis as compared to that of the entire transcriptome
Metabolism
Ribosomal
Proteasome
Cell cycle
Translation
Ubiquitin
Mitochondrial chaperone
Amino Acid Metabolism
Acute HSR (1hour)
Chronic HSR
ER Chaperones
Autophagy
Cytoplasmic chaperones
Proteolysis
Sterol Biosynthesis
Stress Response
Chaperone
Fatty Acid Metabolism
Polyphosphate
TCA cycle
Ubiquitin ligase
Ubiquitin protease
Proteases
sse1Δ
rqc2Δ
hsp82Δ
jjj1Δ
san1Δ
ssa3Δ
egd1Δ
ssa1Δ
ssb1Δ
mcx1Δ
rkr1Δ
hsp104Δ
sti1Δ
ssc1(d)
Median Shift
Median Expression shift of Pathways vs. global transcriptome, FDR=0.05

◂**Fig. 4** **a** Number of differentially upregulated and downregulated genes in the PQC gene deletions were plotted against the number of protein molecules of each PQC (as obtained from [23]). The size of the circle corresponds to the abundance of the PQC in a wild-type cell, refer Fig. 1a (right panel). **b** Mean divergence (in expression of genes) of a random set of genes for each PQC is plotted against the number of protein molecules of each PQC component. Refer to Table S4 for details of divergence calculations. **c** The mean divergence of the set of proteostasis genes (on *X*-axis) is plotted against the mean divergence of a random set of genes (of the same number of genes as that in the proteostasis set) for each PQC deletion, depicted by the red triangles. The black line is the actual regression line. If the PQC deletions had more divergence in the proteostasis set of genes, the triangles would lie below the grey line. (Also see Tables S4, S5). **d** Statistical analysis of expression for gene clusters was done by obtaining genes that belong to specific cellular components and functions. Each cell represents the expression alteration of each group (column header) when compared with the full transcriptome in the same deletion strain (row header). The fold change in their expression values in the PQC deletion strains w.r.t BY4741 (parental strain) was compared to the global alteration in transcripts using Mann–Whitney test. The *p* values obtained were corrected for multiple comparisons using FDR and the cells that did not cross the cut-off significance for *p* value 0.05 are without any colour. The colour scheme is graded from red (down-regulated) to blue (upregulated) showing median fold change values. The size of the circle represents the median fold change shift in either direction

general. Third cluster was found to contain Egd1 and Rqc2 (cluster 3), both of which are associated with ribosomes and are involved in quality control of nascent polypeptides. Interestingly, Rkr1 (Ltn1), known to be associated with Rqc2 (Tae2) was not part of this cluster. Fourth, cytosolic chaperones that aid folding and refolding of aggregates (Hsp104, Ssa3 and Sse1) clustered together (cluster 4).

These correlations were used to obtain a network between the PQCs based on the similarity of transcriptomic response. We overlayed the transcriptomic response network with the epistatic scores between the chaperones and obtained an unexpected dissimilarity between the epistasis scores and response correlations (Fig. 5b). With respect to epistasis, genes in the same pathways are expected to have positive epistatic scores. These pairs, since they are on the same pathways, should also show similar cellular response upon their deletion. However, the positively epistatic pairs do not show a stronger correlation than the negatively epistatic pairs. Strikingly, although Sse1 and Sti1 are strongly exacerbating pairs in terms of epistasis (negative epistatic interaction), they have one of the weakest links in the map. Additionally, many of the non-epistatic pairs (for example, San1 and Rkr1) show the strongest connections in the response map.

Overall there seems to be a weak similarity between the PQC nodes based on their localization and function. This corroborates well with client-dependent response rather than misfolding/aggregation driven one. Despite this, similarities highlight interesting overlaps that are yet to be discovered: connection between Ssb1 and Hsp82, or Rqc2 and Egd1 will be interesting to delineate.

Yeast PQCs are heavily redundant due to genome duplication and are known to have functional redundancies [20, 25]. We asked if the response to PQC deletion led to upregulation of the parallel pathways [26]. To answer this, we investigated the correlation between reported epistasis values (ε) and gene expression [27]. Genetic interactions as obtained through fitness epistasis scores (ε) define functional relationships between pathways; their dependency, and redundancy. Genes with strong negative interactions are usually the ones that operate in parallel although redundant pathway; we expect the pathways parallel to a specific PQC-containing pathway to be upregulated when that PQC is deleted. Given this, we wondered if the cellular response is guided by the genetic interaction network of the PQC genes. We addressed the issue by checking for the correlation between epistasis scores (ε) and the transcriptional response to a PQC deletion and see if the response is guided by the epistatic interactions defined by the chaperone (Fig. S3B). However, we observed no apparent correlation between epistasis scores (ε) and the transcriptome regulation. Thus, the experimentally observed redundant pathways are not upregulated upon deletion of a PQC. The strongest negative genetic interactors are synthetically lethal; even these genes were not upregulated (Fig. 5c). Summarily, the backup pathways, or the parallel pathways are not upregulated when a particular PQC component is absent.

Taken together all of the above results support that the response to PQC gene deletions are guided by missing function of the chaperone–client in the cell and not through sensors of proteostasis. This response possibly compensates for the loss of activity of the clients but not for the loss of proteostasis. This seems to be a fundamentally different from the heat shock response.

To verify if this limitation was specific to PQC gene deletions or true for any gene deletion in *S. cerevisiae*, we took advantage of a recently reported large scale transcriptome study of ~ 700 deletion strains [28]. This allowed us to investigate if transcriptional response to specific deletions is generally uncoupled to epistatic interactions or if this feature was exclusive of the PQC genes. None of the gene deletions, except three (ybl039c, yor209c, ygl252c) show any significant correlation between the transcriptional alterations of the expressed genes and the epistasis of these with the gene that is deleted (Table S7). All the three that show significant correlation exhibit negative correlation between epistasis values and expression change; negatively epistatic genes are upregulated while the positive ones are downregulated. This is exactly as we expected in case optimality is built into the response network. Thus, barring these three exceptions, all the other deletions behave like the PQC component deletions; genes that are negatively epistatic to the deleted

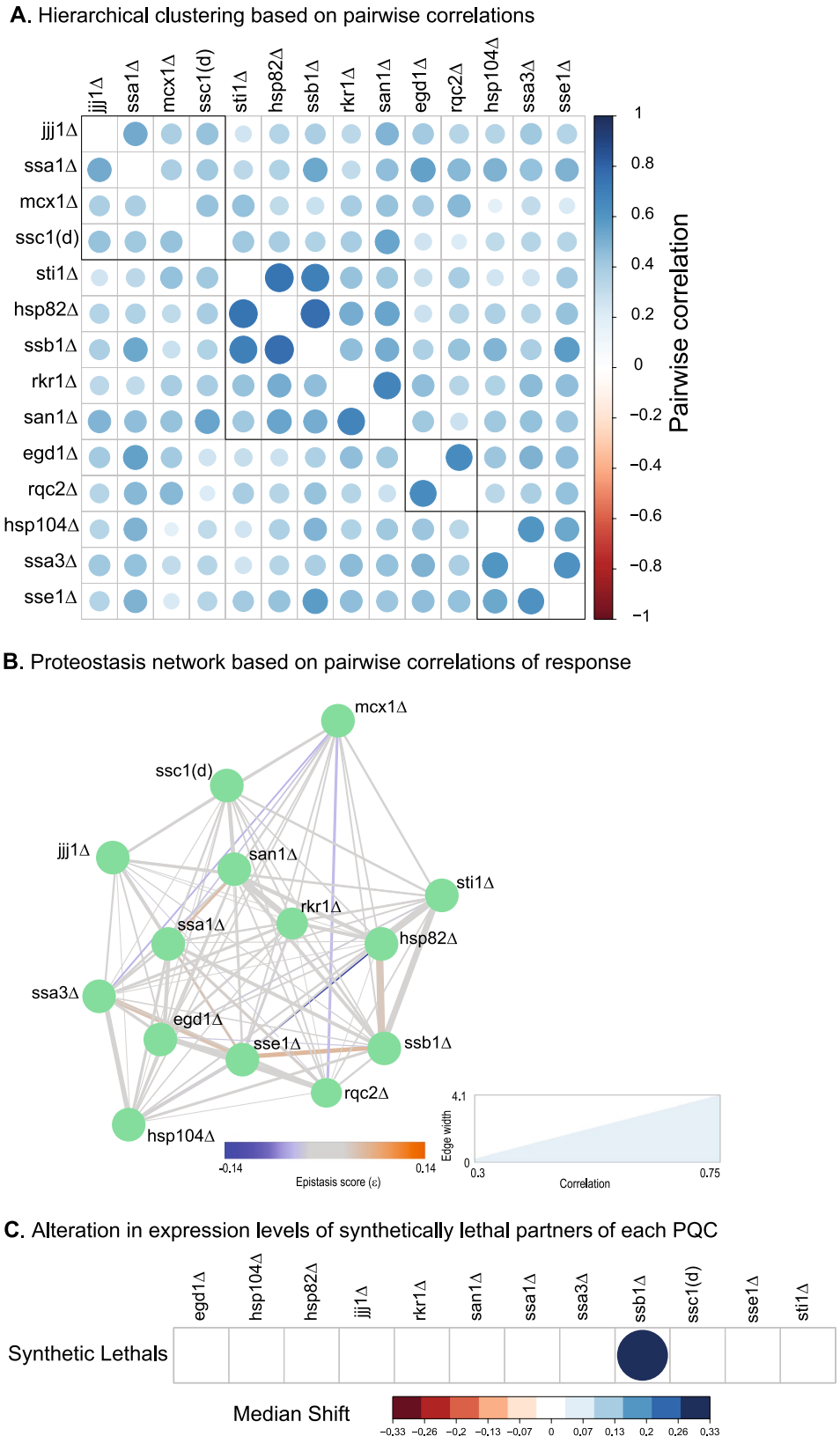

Fig. 5 **a** Hierarchical clustering for PQC genes using the correlations obtained in (S3A). Four clusters are identified and are indicated by black boxes. Bigger circle indicates a stronger correlation. The colours and size of the circle indicate the extent of correlation between the transcriptome profiles of two PQC gene deletions strains. The diagonal elements have a correlation of 1 and are omitted for clarity. **b** The network view of the transcriptomic correlations between PQC deletions. A thicker line indicates stronger correlation than a thinner line. The colour of the line is dictated by the Boone epistasis scores (ε) (27) between the two genes. The three-colour key for epistasis showing blue for negative epistasis (exacerbating interactions), grey indicates zero epistasis (no interaction) and red shows positive epistasis (alleviating interactions). **c** Expression changes of synthetic lethals in each of these PQC gene deletions were compared to that of the entire transcriptome. The fold change in their expression values in the PQC deletion strains w.r.t BY4741 (parental strain) was compared to the global alteration in transcripts using Mann–Whitney test. The p values obtained were corrected for multiple comparisons using FDR and the cells that did not cross the cut-off significance for p value 0.05 are without any colour. The colour scheme is graded from red (down-regulated) to blue (upregulated) showing median fold change values. The size of the circle represents the median fold change shift in either direction

genes, do not show an upregulation. This underlines that response to any perturbation, not limited to the PN, is not guided by the optimality as predicted by the genetic interaction network.

Cryptic optimal pathways can be activated to alleviate PQC deletion associated fitness defects

Since compensatory pathways were not upregulated, we questioned if upregulating or activating such existing compensatory pathways could alleviate the defects arising due to PQC gene deletion. Two PQC gene deletions (jjj1Δ and sse1Δ) showed significant growth defect at physiological temperature of 30 °C (Fig. 1b) and also the strongest perturbation of proteostasis pathways (Fig. 4a–c; Table S4). As a test to check if forced upregulation of a parallel pathway can alleviate defects in a PQC deletion we overexpressed Sse2, a negative genetic interactor of Sse1, in the absence and presence of Sse1. Sse2 overexpression indeed alleviated the growth defect of sse1Δ deletion strain (Fig. 6a; S4A). This demonstrates that cryptic pathways exist, but these are not upregulated optimally to completely take care of the PQC deletion.

However, we did not get fitness alleviation in jjj1Δ when we expressed three of the randomly chosen top negative genetic interactors (asc1, vid22, and vam7) (Fig. S4B). Since all the four proteins work as part of some complex in a pathway, it is apparent that upregulation of only a single gene is not enough to upregulate the cryptic pathway. One of the top negative interactors of jjj1Δ is Stb5 [29] and this encodes a transcription factor that is activated during oxidative stress. To activate Stb5, we gave an oxidative insult to the cells. Remarkably, activation of this branch by treating the cells with a mild concentration of paraquat (Pq) could alleviate the growth phenotype of jjj1Δ (Fig. 6b). Conversely, when we treated cells with an anti-oxidant, ascorbate, we found growth of jjj1Δ to be mildly affected (Fig. 6c). To verify, we chose another condition where cells face oxidative stress. A mild but chronic heat shock treatment does result in activation of oxidative stress response pathways [30, 31]. Thus, during a chronic heat shock treatment (at 37 °C), we found the growth defect of jjj1Δ to be alleviated (Fig. 6d). Hence, cryptic pathways could be activated to rescue defects due to the tested PQC gene deletions. This also demonstrates that fitness compensation is dependent upon activation of redundant pathways rather than a single gene upregulation.

To further check if proteostasis defect of jjj1Δ is also alleviated by upregulating the oxidative stress response pathway, we monitored the stability of the metastable TS22 protein upon paraquat treatment. Reassuringly, TS22 was more stable in jjj1Δ in the presence of oxidative stress than in the absence of the stress (Fig. 6e). This was true only for jjj1Δ and not BY4741, the WT background strain where we find the metastable protein, TS22, was not stabilized in the presence of oxidative stress, as it was in jjj1Δ. Commensurately, the activity of TS22, but not WT Nat-R, was marginally higher in jjj1Δ in the presence of Pq than in its absence (Fig. 6f; S4D). Better folding of TS22 in jjj1Δ in the presence of oxidative stress is supported by the evidence that jjj1Δ strains harbouring TS22 mutant of Nat-R could grow significantly better (at CloNAT concentration of 25 µg/ml, $p < 0.05$) and marginally better (at CloNAT of 50 and 100 µg/ml, $p < 0.1$) in the presence of Pq than its absence. This is in stark contrast to BY4741, where oxidative stress led to a significant decrease in the activity (and thereby growth) of TS22. Oxidative stress response pathway that shows interaction at the genetic level, could be activated to compensate for the absence of jjj1. However, a naturally evolved *S. cerevisiae* cell has not linked these two pathways to compensate for the absence. Taken together, the above examples demonstrate that cellular systems do have the capability to take care of the short-comings, but this capability is not switched on by default upon depletion of the gene.

Implications

Proteostasis network, like all other cellular networks, has a complex architecture that needs to be understood to tackle problems that are associated with its collapse. Proteostasis collapse is a hallmark of ageing and is also associated with many late-onset diseases [32, 33]; alleviation of its collapse has the potential to delay progressive ageing and age-associated diseases. Many of the polyglutamine-mediated late-onset diseases are associated with collapse of proteostasis. Although polyglutamine stretches lead to protein aggregation and sequestration of crucial chaperones the cells do not mount a stress response to correct this; it is believed that polyglutamines act dominantly to inhibit heat shock response and thereby limit cellular capacity to restore proteostasis. The fact that earlier reports do not find HSR to be activated upon aggregation of mutant polyQ species [16], may have little to do with toxicity of these proteins. Here using different models of chaperone and other PQC component deletions we show that at least *S. cerevisiae* (where polyglutamine toxicity is conserved) is unable to restore proteostasis upon chaperone depletion even in the absence of any exogenous polyglutamine aggregates. This clearly shows that cellular response to chaperone depletions is non-optimal; polyglutamine stretches' role in suppressing heat shock response may not be a crucial contributor in its toxicity. Limitation of cellular ability to restore proteostasis may be one of the reasons why cells are unable to handle ageing and misfolding-associated problems.

Interestingly, our results on the effect of celastrol on a metastable protein shows that heat shock response may

A. Fitness defects of sse1 Δ is rescued by sse2 over-expression at 30°C

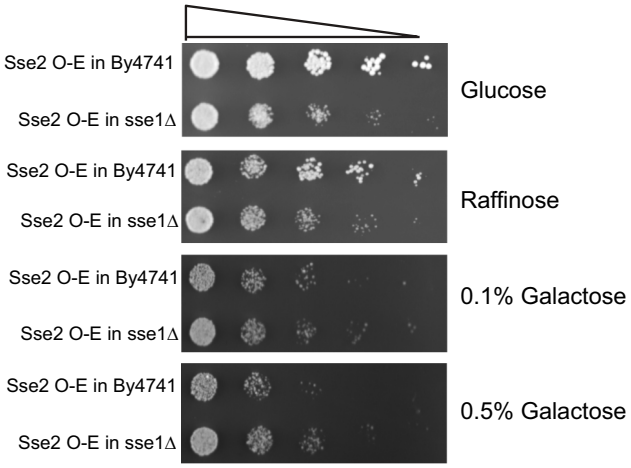

B. Fitness defect of jjj1 Δ is rescued during growth in presence of oxidative stress at 30°C

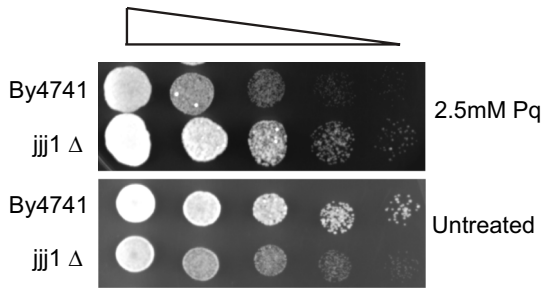

C. Fitness defect of jjj1 Δ is enhanced in presence of ascorbate at 30°C

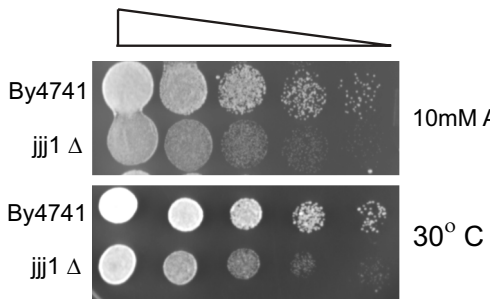

D. Fitness defects of jjj1 Δ is rescued during growth at 37 °C

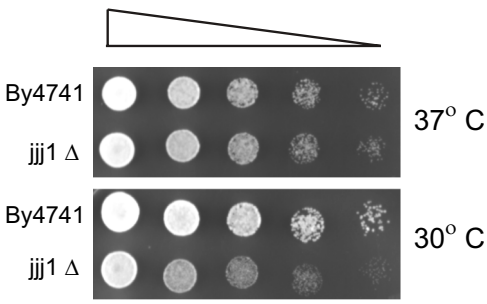

E. Proteostasis capacity is better in jjj1 Δ upon oxidative stress

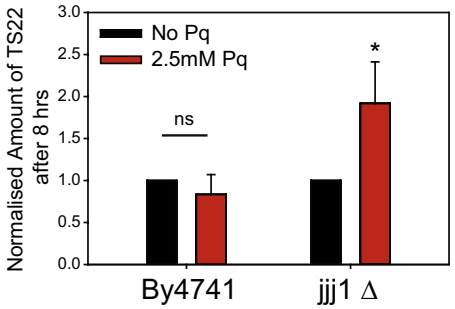

F. Proteostasis capacity is better in jjj1Δ with oxidative stress

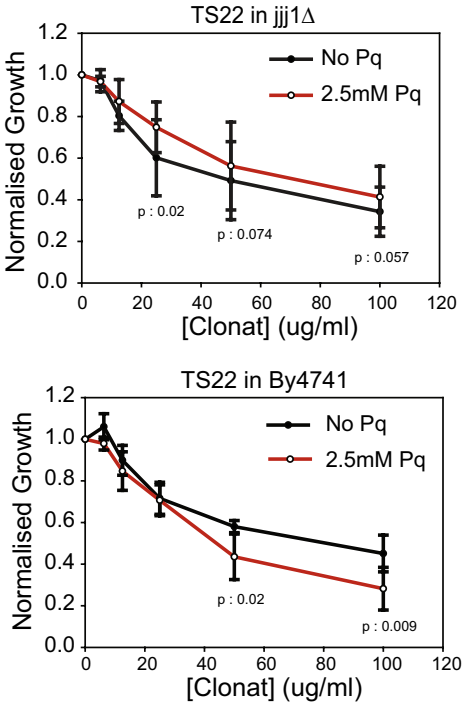

◂**Fig. 6** **a** By4741 and sse1Δ bearing galactose-inducible over expression of Sse2 were spotted on YPD, YP + Raffinose or YP + Galactose and grown at 30 °C. Representative images shown. **b** BY4741 and jjj1Δ were spotted on YPD agar plates in the presence (upper panel) or absence (lower panel) of 2.5 mM Paraquat and grown at 30 °C to assay growth fitness of the strains. Representative images shown. **c** BY4741 and jjj1Δ were spotted on YPD agar in the presence (upper panel) or absence (lower panel) of 10 mM ascorbate and grown at 30 °C. Representative images shown. **d** BY4741 and jjj1Δ were spotted on YPD agar plates and grown at 37 °C (upper panel) and control grown at 30 °C (lower panel). **e** Quantification of western blotting of TS22 in BY4741 and jjj1Δ with or without 2.5 mM Paraquat (refer S4C) ($n = 3$). **f** Activity of TS22 measured in terms of growth in varying concentrations of the antibiotic Clonat, in jjj1Δ (left panel) and BY4741(right panel) with or without 2.5 mM Paraquat (also refer Fig. S4D). p values, as calculated by paired student's t test, are mentioned below the error bars. In all figures, $*p < 0.05$, $**p < 0.01$, $***p < 0.001$

not contribute constructively towards efficient folding of a metastable protein. Thus, heat shock response may not be the pathway of choice to target when aiming to efficiently fold mutant proteins, while it may still be a pathway of choice for mitigating toxicity associated with misfolding or aggregation [17, 34, 35].

Although the work reported here is done on *S. cerevisiae*, and with single deletions of chaperones, it is likely to hold true for more complex organizational structures in mammals. It is also likely that the response pattern and efficiency is dependent on cell and tissue-type dependent on the background response pathways. Only further work in this direction will be able to substantiate the findings and their generality. Since this work is based on PQC gene deletions and not partial depletion it may not correctly represent scenarios where chaperones are sequestered. However, deletions represent the extreme limit of depletion of a protein; it is therefore unlikely that cellular response dormant even after deletion will be switched on upon partial depletion of the protein. Summarily, this study unravels a cryptic limitation in the yeast chaperone network, a proposal that needs further investigation in higher organisms.

Materials and methods

Media and growth conditions

Rich media for culturing yeast (YPD medium) containing 1% (w/v) yeast extract, 2% (w/v) peptone and 2% (w/v) dextrose. Yeast strains BY4741 (leu2Δ0 ura3Δ0 met15Δ0 his3Δ1) and deletion strains in the background of BY4741 (*Saccharomyces* Genome Deletion Project, http://www-sequence.stanford.edu/group/yeast_deletion_project/deletions3.html) (Open biosystems, GE Healthcare) were grown at 30 °C, 200 rpm.

Cells were inoculated in YPD at 0.1 O.D. 600 from an overnight primary culture and grown to mid-log phase before harvesting for RNA isolation.

RNA sequencing for each strain was performed in two biological replicates.

Growth phenotype by spotting

From overnight primary culture in YPD, cells were inoculated in YPD at 0.1 O.D. and allowed to grow at 30 °C, 200 rpm they reached an O.D. of 0.6–0.7 thereafter, they were serially diluted (starting with an O.D. of 0.5) by a factor of 10 and 5 µl of each dilution was spotted on YPD plates that either contained a stressor of did not. These plates were then kept at 30 °C for 48 h; except in the case of heat shock, they were incubated at 37 °C. Over-expression plasmids for Sse1, Sse2, Vid22, Asc1 and Vam7 [36] were obtained from Dharmacon.

Making temperature sensitive (TS) mutants of Nat-R

Nat-R gene was cloned under Tef2 promoter in pRS316 vector. Nat-R was amplified from pYM-N17 along with its promoter. DsRed was amplified from pYM35 by adding *Ecor*I at 5′ and *Sac*I at 3′ end. Nat-R and DsRed were fused by the help of *Ecor*I enzyme; by removing the stop codon from Nat-R. The entire construct of Tef2 promoter driven Nat-R fused to DsRed along with its 3′ UTR was cloned within the restriction sites *Hind*III and *Sac*I.

TS22 has the following mutations in it: E49G, V52M and D110V.

Cells bearing WT Nat-R or TS22 were always grown in synthetic media deficient of uracil (SD-ura).

Making temperature sensitive mutants of yeGFP

yeGFP was cloned in pRS316 under GPD promoter and cyc1 terminator. The entire construct of GPD–GFP–cyc1 has been introduced into the vector between Sac1 and Kpn1 sites. M1 has the mutation K45E and M8 has the mutations G24C, V219S.

Cells bearing WT GFP or M1 or M8 were always grown in synthetic media deficient of uracil (SD-ura).

Western blotting

Secondary culture was inoculated at ~ 0.1 O.D. and grown at 30 °C; 200 rpm. After 6 h of growth, the cultures were pelleted. Protein was isolated by alkaline lysis method, concentration was estimated by BCA (Thermo Scientific, USA) and 30 µg of total protein was loaded per lane in a 10% gel. The nitrocellulose membrane was probed with custom anti-Nat-r primary antibody (1:5000 dilution). In case of GFP, primary

antibody used was AB290 from abcam (1:10,000 dilution). A horseradish peroxidase-conjugated goat anti-rabbit antibody (sc-2030, Santa Cruz Biotechnology, Inc. USA) was used as secondary antibody and developed through chemiluminescence (Immobilon Western Chemiluminescent HRP Substrate, Merck Millipore). Blots were quantitated using ImageJ and were normalized to ponceau with its respective blot.

For celastrol treatment, 20 μM was used to treat cells for 6 h while growing in secondary culture.

For cycloheximide (chx) chase, cells were inoculated at ~ 0.1 O.D. and grown at 30 °C; 200 rpm in secondary culture. After 4 h of growth, cycloheximide (0210018305, MP Biomedicals) was added to a final concentration of 40ug/ml and aliquots collected (on ice) and mentioned time intervals. These cultures were then pelleted, protein isolated and processed for western blotting.

Growth assay

From an overnight primary culture, cells were grown in 96-well, deep-well plates for the assay with varying concentrations of the antibiotic CloNat (nourseothricin; AB102XL from Lexy NTC). 400 ul of culture (initial O.D. being 0.05) was kept per well and grown at 30 °C; 200 rpm for 12 h. Growth readings were taken on a multi-plate reader (TECAN). Growth assay was performed similarly with AZC (L-Azetidine-2-carboxylic acid; A0760 Sigma).

Flow cytometry

Cells were grown till saturation in primary culture and then inoculated at 0.1 O.D. in secondary culture. This was grown for 6 h at 30 °C with shaking; post which, they were diluted with 1× PBS and injected directly to a LSRII flow cytometer (BD).

FACS DiVA 6.2 (BD) was used to record the data into ".fcs3.0" files. GFP was excited at 488 nm and fluorescence was collected through a 505-nm long-pass filter and a 515/20 band-pass filter.

RNA preparation

Cells were lysed using acid-washed glass bead and total RNA was extracted by TRIzol (Invitrogen) method. It was further purified using Qiagen columns (RNeasy mini kit). RNA concentration and integrity were determined using nanodrop and agarose gel electrophoresis.

Library preparation

Using Truseq RNA sample prep kit v2 (stranded mRNA LT kit), the library was prepared according to the manufacturer's instructions (www.illumina.com). 700 ng of RNA from each sample was used to generate the library. Adaptor-ligated fragments were purified using AMPure XP beads (Agencourt). Adaptor-ligated RNAseq libraries were amplified (12–14 cycles), purified and measured with a Qubit instrument (Invitrogen). The average fragment size of the libraries was determined with a BioAnalyzer DNA1000 LabChip (Agilent Technologies). Diluted libraries were multiplex-sequenced and run on a HiSeq2000 Illumina platform in HiSeq Flow Cell v3 (Illumina Inc., USA) using TruSeq SBS Kit v3 (Illumina Inc., USA) for cluster generation as per manufacturer's protocol.

Mapping sequence reads

Only reads with phred quality score equal or higher than 30 were taken for analysis. Trimmomatic (v0.43) [37] was used to trim read sequences. Reads were then aligned to the transcriptome of *S. cerevisiae* strain S288c as available from ENSEMBL using Kallisto (v0.36) software [38]. The reads on an average had over 80% alignment with the reference genome. Gene expression levels were estimated as TPM (transcripts per million) values. The estimated counts were combined into a matrix and analysed with EBSeq v1.10.0. Differential expression tests are run using EBTest with 20 iterations of the EM algorithm [39]. After this, the list of differentially expressed genes, $\log_2$ fold change of all the genes in the transcriptome and the posterior probabilities of being differentially expressed are obtained using GetDEResults with method "robust", FDR method "soft" FDR 0.05, threshold FC 0.7, threshold FC ratio 0.3.

Construction of the co-regulation network and hierarchically clustered corrgrams

To examine the similarity of the transcriptomic response to chaperone deletions, we computed the pairwise correlation co-efficient of $\log_2$ fold changes of all the genes (complete transcriptome) across all the strains. Here, the correlation co-efficient indicates the extent of similarity of the transcriptomic response across mutants to the loss of the chaperone (1 being most similar and 0 being least similar). The correlation matrix was converted into a network with nodes representing the mutants and the edges weighted by the correlation between the mutants. A force directed layout (implemented through Cytoscape [40]) was then applied on the network which clustered strongly connected nodes towards the centre and repelled weakly connected nodes to the periphery of the network. The nodes of the network show the structure of the protein, if available and were taken from STRING database [41]. A complementary representation involves hierarchically clustering of a heatmap of the correlation values.

Proteostasis pathways, and HSR expression shift analysis

To detect shifts in expression for pathways, we employed a GO pathway/functional category based analysis strategy that tests for the overall shift in expression levels for a group of genes that belong to a pathway (obtained from YeastMine) against the rest of the genes in the transcriptome. Refer to Table S4 for details of genes used for each category. For the category 1 h heat shock response (HSR), we took the first 45 genes upregulated upon 60 min heat shock treatment at 37 °C by analysing a previously published microarray data [30]. For 6-h chronic HSR, we took the top 40 genes from our data, upon growing BY4741 at 37 °C for 6 h (till mid-log phase). The non-parametric Mann–Whitney test is used to avoid issues with over-dispersion in the data and to test the significance of the median shift in expression of genes in a particular pathway in comparison to the whole transcriptome. The Benjamini–Hochberg correction is applied when testing in a combinatorial fashion across pathways to correct for multiple testing.

Besides GO pathways we followed the same strategy to examine the expression status of physically interacting partners, co-chaperone genes, and synthetic lethal partners. The list of physical interacting partners for each protein was obtained from BIOGRID [42]. All statistical tests and analysis were performed with R version 3.3.0 [43] scatterplot matrices using the lattice package and heatmaps were made using the corrplot package [44].

Transcription–epistasis correlation

We downloaded the transcriptome fold changes as provided in the supplementary files by in a recent report by Kemmeren et al. [28], and mapped the deletion from the columns in the provided dataset to deletions in the epistasis score matrix and extracted their epistasis profiles. 511 mutants out of the 700 mutants mapped to the epistasis score matrix. For each deletion, we computed the correlation co-efficient with significance indicated by p values between the transcriptome fold changes of genes to the epistasis score within the epistasis profile.

Calculating divergence

Please refer to Table S4. We calculated fold change of all the transcripts with respect to BY4741 for each of the deletion strains. The proteostasis component genes were defined as in Table S5. For each deletion strain, from the whole transcript sample, we calculated the fold change distribution for 10,000 sets of randomly picked genes (with replacement) to match the number of proteostasis genes (611). As a measure of divergence of the distribution, Shannon entropy was calculated for each of these 10,000 distributions, the mean of the Shannon entropy and the standard deviation were obtained. Shannon entropy was also calculated for the proteostasis components. Difference between the Shannon entropies was obtained calculated. Negative value indicates lower divergence in proteostasis components. p values were obtained using z test. In all the deletion strains, proteostasis components have lower divergence than a randomly chosen subset of the same number of genes, and this difference is statistically significant.

Note: For each case, to calculate Shannon entropy we obtained a normalized histogram with 121 bins ranging from − 3 to 3 of log2 of fold change values. The area of the histogram was normalized to 1. The fraction in each histogram was read directly as the probability of finding genes in a particular (ith) bin (pi). Shannon entropy was obtained by taking a summation of $-\text{pi} \times \log(\text{pi})$ for all the bins. 0 would indicate lowest entropy state, in case all genes were in the same bin. The value will increase in case the distribution is spread out, in other words if the divergence of the distribution is high.

Acknowledgements We are grateful to Dr. Mohammed Faruq for aiding us with the Illumina sequencing platform. We thank Dr. Deepak Sharma (affiliated to CSIR-IMTECH) for assistance with reagents. This work was primarily funded by OLP1104 grant by CSIR to KC and partially by the grant YSS/2015/000532 from SERB to KM along with SNU core funding. We thank the HPC facility of CSIR-IGIB, for aiding us with computing resources. AG1 (Asmita), AG2 (Abhilash) and LM thank UGC for their fellowship. MV is grateful to CSIR, SD to SNU-core funding, and DPD to DBT for their fellowships.

Author contributions AG1 and KC designed the work. KC, KM and DD supervised the work and analysis. Sequencing was done by AG1. LM made the TS mutants of Nat-R. DPD made Mutants of yeGFP. AG1, SD, MV did the yeast experiments. The transcriptomics experiments were done by AG1. Analysis was primarily done by AG2 along with AG1 and KC. AG1 and KC wrote the manuscript with input from all authors. All authors read and approved the final version of the manuscript.

Compliance with ethical standards

Conflict of interest Authors declare no competing interests.

References

1. Daughdrill GW, Pielak GJ, Uversky VN, Cortese MS, Dunker AK (2005) Natively disordered proteins. Protein folding handbook, pp 275–357. https://doi.org/10.1002/9783527619498.ch41
2. Oldfield CJ, Dunker AK (2014) Intrinsically disordered proteins and intrinsically disordered protein regions. Annu Rev Biochem 83:553–584
3. Kramer G, Boehringer D, Ban N, Bukau B (2009) The ribosome as a platform for co-translational processing, folding and

targeting of newly synthesized proteins. Nat Struct Mol Biol 16(6):589–597
4. Zhang G, Ignatova Z (2011) Folding at the birth of the nascent chain: coordinating translation with co-translational folding. Curr Opin Struct Biol 21(1):25–31
5. Hartl FU, Bracher A, Hayer-Hartl M (2011) Molecular chaperones in protein folding and proteostasis. Nature 475(7356):324–332 **Epub 2011/07/22**
6. Kim YE, Hipp MS, Bracher A, Hayer-Hartl M, Hartl FU (2013) Molecular chaperone functions in protein folding and proteostasis. Annu Rev Biochem 82:323–355 **Epub 2013/06/12**
7. Frydman J (2001) Folding of newly translated proteins in vivo: the role of molecular chaperones. Annu Rev Biochem 70:603–647 **Epub 2001/06/08**
8. Klaips CL, Jayaraj GG, Hartl FU (2018) Pathways of cellular proteostasis in aging and disease. J Cell Biol 217(1):51–63 **(Epub 2017/11/12)**
9. Wolff S, Weissman JS, Dillin A (2014) Differential scales of protein quality control. Cell 157(1):52–64
10. Macario AJ, de Macario EC (2005) Sick chaperones, cellular stress, and disease. N Engl J Med 353(14):1489–1501
11. Park S-H, Kukushkin Y, Gupta R, Chen T, Konagai A, Hipp MS et al (2013) PolyQ proteins interfere with nuclear degradation of cytosolic proteins by sequestering the Sis1p chaperone. Cell 154(1):134–145
12. Wang X, Venable J, LaPointe P, Hutt DM, Koulov AV, Coppinger J et al (2006) Hsp90 cochaperone Aha1 downregulation rescues misfolding of CFTR in cystic fibrosis. Cell 127(4):803–815
13. Koulov AV, LaPointe P, Lu B, Razvi A, Coppinger J, Dong M-Q et al (2010) Biological and structural basis for Aha1 regulation of Hsp90 ATPase activity in maintaining proteostasis in the human disease cystic fibrosis. Mol Biol Cell 21(6):871–884
14. Gong Y, Kakihara Y, Krogan N, Greenblatt J, Emili A, Zhang Z et al (2009) An atlas of chaperone-protein interactions in *Saccharomyces cerevisiae*: implications to protein folding pathways in the cell. Mol Syst Biol 5:275 **(Epub 2009/06/19)**
15. David DC, Ollikainen N, Trinidad JC, Cary MP, Burlingame AL, Kenyon C (2010) Widespread protein aggregation as an inherent part of aging in *C. elegans*. PLoS Biol 8(8):e1000450 **(Epub 2010/08/17)**
16. Labbadia J, Cunliffe H, Weiss A, Katsyuba E, Sathasivam K, Seredenina T et al (2011) Altered chromatin architecture underlies progressive impairment of the heat shock response in mouse models of Huntington disease. J Clin Investig 121(8):3306–3319
17. Katsuno M, Sang C, Adachi H, Minamiyama M, Waza M, Tanaka F et al (2005) Pharmacological induction of heat-shock proteins alleviates polyglutamine-mediated motor neuron disease. Proc Natl Acad Sci 102(46):16801–16806
18. Zhou H, Li S-H, Li X-J (2001) Chaperone suppression of cellular toxicity of huntingtin is independent of polyglutamine aggregation. J Biol Chem 276:48417–48424. https://doi.org/10.1074/jbc.M104140200
19. Stenoien DL, Cummings CJ, Adams HP, Mancini MG, Patel K, DeMartino GN et al (1999) Polyglutamine-expanded androgen receptors form aggregates that sequester heat shock proteins, proteasome components and SRC-1, and are suppressed by the HDJ-2 chaperone. Hum Mol Genet 8(5):731–741
20. Kabani M, Martineau CN (2008) Multiple hsp70 isoforms in the eukaryotic cytosol: mere redundancy or functional specificity? Curr Genom 9(5):338–348 **(Epub 2009/05/28)**
21. Werner-Washburne M, Stone DE, Craig EA (1987) Complex interactions among members of an essential subfamily of hsp70 genes in *Saccharomyces cerevisiae*. Mol Cell Biol 7(7):2568–2577
22. Meyer AE, Hung NJ, Yang P, Johnson AW, Craig EA (2007) The specialized cytosolic J-protein, Jjj1, functions in 60S ribosomal subunit biogenesis. Proc Natl Acad Sci USA 104(5):1558–1563 **(Epub 2007/01/24)**
23. Ghaemmaghami S, Huh WK, Bower K, Howson RW, Belle A, Dephoure N et al (2003) Global analysis of protein expression in yeast. Nature 425(6959):737–741 **(Epub 2003/10/17)**
24. Brandman O, Stewart-Ornstein J, Wong D, Larson A, Williams CC, Li G-W et al (2012) A ribosome-bound quality control complex triggers degradation of nascent peptides and signals translation stress. Cell 151(5):1042–1054
25. Sharma D, Masison DC (2008) Functionally redundant isoforms of a yeast Hsp70 chaperone subfamily have different antiprion effects. Genetics 179(3):1301–1311
26. Blatch GL, Edkins AL (2014) The networking of chaperones by co-chaperones: control of cellular protein homeostasis. Springer, Berlin
27. Costanzo M, VanderSluis B, Koch EN, Baryshnikova A, Pons C, Tan G et al (2016) A global genetic interaction network maps a wiring diagram of cellular function. Science 353(6306):1420 **(Epub 2016/10/07)**
28. Kemmeren P, Sameith K, van de Pasch LA, Benschop JJ, Lenstra TL, Margaritis T et al (2014) Large-scale genetic perturbations reveal regulatory networks and an abundance of gene-specific repressors. Cell 157(3):740–752 **(Epub 2014/04/29)**
29. Usaj M, Tan Y, Wang W, VanderSluis B, Zou A, Myers CL et al (2017) TheCellMap.org: a web-accessible database for visualizing and mining the global yeast genetic interaction network. G3 (Bethesda) 7(5):1539–1549 **(Epub 2017/03/23)**
30. Gasch AP, Spellman PT, Kao CM, Carmel-Harel O, Eisen MB, Storz G et al (2000) Genomic expression programs in the response of yeast cells to environmental changes. Mol Biol Cell 11(12):4241–4257
31. Davidson JF, Whyte B, Bissinger PH, Schiestl RH (1996) Oxidative stress is involved in heat-induced cell death in *Saccharomyces cerevisiae*. Proc Natl Acad Sci 93(10):5116–5121
32. Taylor RC, Dillin A (2011) Aging as an event of proteostasis collapse. Cold Spring Harbor Perspect Biol. https://doi.org/10.1101/cshperspect.a004440
33. Kaushik S, Cuervo AM (2015) Proteostasis and aging. Nat Med 21(12):1406–1415 **(Epub 2015/12/10)**
34. Magrané J, Smith RC, Walsh K, Querfurth HW (2004) Heat shock protein 70 participates in the neuroprotective response to intracellularly expressed β-amyloid in neurons. J Neurosci 24(7):1700–1706
35. Sõti C, Nagy E, Giricz Z, Vígh L, Csermely P, Ferdinandy P (2005) Heat shock proteins as emerging therapeutic targets. Br J Pharmacol 146(6):769–780
36. Gelperin DM, White MA, Wilkinson ML, Kon Y, Kung LA, Wise KJ et al (2005) Biochemical and genetic analysis of the yeast proteome with a movable ORF collection. Genes Dev 19(23):2816–2826
37. Bolger AM, Lohse M, Usadel B (2014) Trimmomatic: a flexible trimmer for Illumina sequence data. Bioinformatics 30(15):2114–2120 **(Epub 2014/04/04)**
38. Bray NL, Pimentel H, Melsted P, Pachter L (2016) Near-optimal probabilistic RNA-seq quantification. Nat Biotechnol 34(5):525–527 **(Epub 2016/04/05)**
39. Leng N, Dawson JA, Thomson JA, Ruotti V, Rissman AI, Smits BM et al (2013) EBSeq: an empirical Bayes hierarchical model for inference in RNA-seq experiments. Bioinformatics 29(8):1035–1043 **(Epub 2013/02/23)**
40. Smoot ME, Ono K, Ruscheinski J, Wang PL, Ideker T (2011) Cytoscape 2.8: new features for data integration and network visualization. Bioinformatics 27(3):431–432 **(Epub 2010/12/15)**

41. Szklarczyk D, Franceschini A, Kuhn M, Simonovic M, Roth A, Minguez P et al (2011) The STRING database in 2011: functional interaction networks of proteins, globally integrated and scored. Nucleic Acids Res 39(Database issue):561–568 **(Epub 2010/11/04)**
42. Oughtred R, Chatr-aryamontri A, Breitkreutz BJ, Chang CS, Rust JM, Theesfeld CL et al (2016) BioGRID: a resource for studying biological interactions in yeast. Cold Spring Harbor Protocols 2016(1):pdb top080754 **(Epub 2016/01/06)**
43. Team RC (2014) R: a language and environment for statistical computing. R Foundation for Statistical Computing, Vienna, p 2014
44. Wei T, Simko V (2013) corrplot: Visualization of a correlation matrix. R Package Version 073 230(231):11